

6 Telescopes for visible light

Astronomers use telescopes to collect radiation from astronomical sources and to estimate their direction and structure as well as spectral and absolute intensities. The wide range of photon energies involved in astronomical observations means that the telescopes are very different in form depending on wavelength band. We can subdivide telescope types roughly into four categories.

- detectors which sense the direction of arrival and energy of individual (gamma-ray) photons
- non-focusing (X-ray) collimators which restrict the field of view of the detector
- phased arrays, and pencil beam interferometers (metre wavelength)
- reflecting or refracting telescopes which focus incoming radiation (all wavelengths except gamma-rays)

Here we will concentrate on the latter category, and especially to those telescopes used to observe visible and infra-red radiation.

The theoretical consideration of resolution that we discussed in previous lectures is only applicable if the lens or mirror as well as the intervening atmosphere is of sufficient optical quality that the image is not already degraded beyond the diffraction limit. There are many effects that will blur an image and these are collectively known as aberrations. With one exception they can all effect images produced by both lenses or mirrors. The universal or monochromatic aberrations are known as the Seidel aberrations. The exception is chromatic aberration and the related second order effects of transverse chromatic aberration and secondary color, and these only effect lenses.

6.1 Lenses, mirrors and geometric optics

The speed of light in a vacuum is a constant, c , identical for all observers. The *phase velocity* v of light in a dielectric medium such as air, water, or glass is always less than c such that

$$n(\lambda) = \frac{c}{v(\lambda)}$$

where n is the *index of refraction*, which in general is a function of the wavelength λ . Another important characteristic of a material is thus the *chromatic dispersion* $dn/d\lambda$. Glassmakers traditionally express this dispersion as the Abbe number, or *costringence*, defined in equation 2, which depends roughly on the reciprocal of the dispersion.

Along a ray of light moving through a medium (a homogenous medium will have straight rays of light) one can measure the distance s that light moves in time t

$$s = \frac{ct}{n}$$

Points of equal s delineate a surface called the *geometrical wavefront*. Wavefronts are always perpendicular to rays. If ds is an infinitesimal element along a ray path the ray travel time is

$$\tau = \int \frac{ds}{v} = \frac{1}{c} \int n ds = \frac{w}{c}$$

where w is the *optical path length*. In some situations with a coherent source (where all waves are emitted in phase) the geometrical wavefronts also correspond to surfaces of equal phase.

6.1.1 Fermat's principle and Snell's law

Fermat's principle states that the path of a ray between two points will always be an extremum in total travel time τ or optical path length.

Consider a situation where a plane separates two different materials, and assume that the index of refraction is larger in the material on the right. A light ray that travels towards the right will strike the normal to the surface at the *angle of incidence*, θ_1 , and the ray splits into two components - a reflected ray, and a refracted ray. These two rays make angles θ_R and θ_2 with the normal, which is measured so that positive angles counterclockwise from the normal.

Fermat's principle implies the law of reflection

$$\theta_1 = -\theta_R.$$

We can also deduce the path of the refracted ray by requiring the optical path between two fixed points P_1 and P_2 to be an extremum. This argument leads to Snell's law of refraction

$$n_1 \sin \theta_1 = n_2 \sin \theta_2 \quad (1)$$

(Note that this expression reduces to the law of reflections for $n_1 = -n_2$.)

Exercise

1. Show that Snell's law and the law of reflections follow from Fermat's principle. (Hint: set up an expression for the optical path length between two points as a function of, for example x and y , and minimize the expression, *i.e.* find $d/dy = 0$, keeping the positions $x_{1,2}$ constant.)

For a ray coming from a medium with a larger index of refraction there is a *critical angle* which produces a refracted ray that never leaves the medium, which one can see is given by

$$\theta_C = \sin^{-1} \left(\frac{n_1}{n_2} \right)$$

This state of affairs is called a *total internal reflection*, where the angle of incidence is greater than θ_C , where all light that reaches the interface is reflected back into the higher index medium.

Snell's law is a general result that applies to any shape, and can be used as the foundation of almost all geometrical optics.

6.1.2 Reflection and transmission coefficients

The laws governing the relative *intensities* of incident and reflected, refracted beams are complicated and fall outside the realm of geometrical optics. *Fresnel's formulas* for reflection and transmission coefficients give the amplitudes of the reflected and refracted waves as a function of angle of incidence, polarization, and indices of refraction. A few results are worth stating:

- Polarization is important. Waves polarized with the electric field vector perpendicular to the plane of incidence (transverse electric phase), are reflected differently than waves polarized with the magnetic field perpendicular to the plane of incidence (transverse magnetic).
- The reflectance, R , is the fraction of the power of the incident wave that is reflected. At normal incidence ($\theta_1 = 0$) and for all cases

$$R = \left(\frac{n_1 - n_2}{n_1 + n_2} \right)^2$$

- For both transverse electric and transverse magnetic polarization the reflectance becomes large at large angles of incidence. In the external case, $R \rightarrow 1.0$ as $\theta_1 \rightarrow 90^\circ$ and light rays that strike a surface at grazing incidence close to 90° will be mostly reflected. For the internal case, $R = 1.0$ for all angles greater than the critical angle.
- For all values of θ_1 other than those described above R is smaller for transverse magnetic than for transverse electric polarization. Thus initially unpolarized light become partially polarized after reflection from a dielectric surface. At one particular angle, *Brewster's angle* $\theta_p = \tan^{-1}(n_1/n_2)$, $R = 0$ for transverse magnetic polarization and only one polarization is reflected.

6.1.3 Reflection from a spherical surface

Consider a concave spherical surface with radius R and center C as shown in figure 1. The line that is coincident with the axis of symmetry (goes through C and the center of the surface) is called the *optical axis*. Set up a Cartesian coordinate system where the z -axis lies on the optical axis and the origin, the *vertex* (V) is at the point where the surface meets the optical axis. Let us describe the situation in the $y - z$ plane. The *paraxial approximation* assumes that all incident rays are nearly parallel to the optical axis, and that all angles of reflection are small. This latter means that the diameter of the mirror is small compared to the radius of curvature.

Consider the ray that originates at the *object* at point O on the optical axis and is reflected at point P to reach the image at I . If the point P is at position

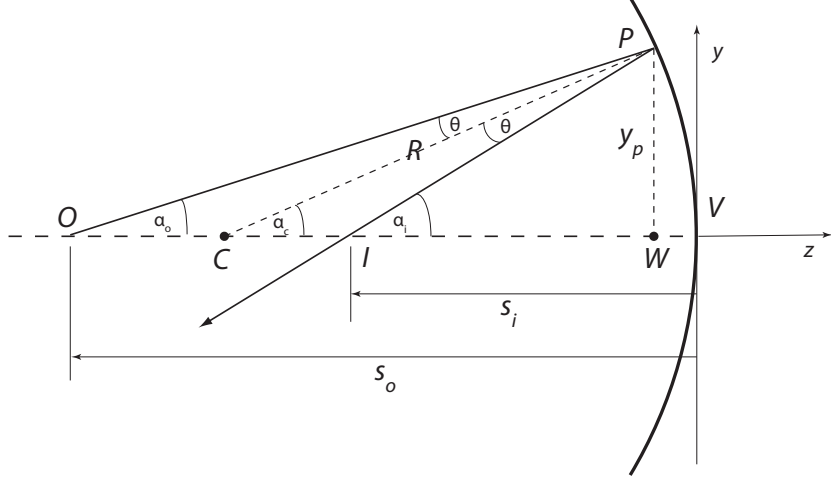


Figure 1: Reflection from a spherical surface. See text for details.

y_p then we can deduce that

$$\begin{aligned}\alpha_o &\approx \tan \alpha_o \approx \frac{y_p}{s_o} \\ \alpha_c &\approx \tan \alpha_c \approx \frac{y_p}{R} \\ \alpha_i &\approx \tan \alpha_i \approx \frac{y_p}{s_i}\end{aligned}$$

given that s_o is the distance between the mirror surface and the object, and s_i is the distance between the image and the mirror surface (both along the optical axis). The angle α_c is the angle between the line joining the center of the surface C and the point P and the optical axis.

If θ is the angle of incidence then we have, considering the triangles OPC and CPI that

$$\theta = \alpha_c - \alpha_o = \alpha_i - \alpha_c$$

or

$$2\alpha_c = \alpha_o + \alpha_i$$

Substituting this into the first three approximations for the angles we derive

$$\frac{2}{R} = \frac{1}{s_o} + \frac{1}{s_i} = \frac{1}{f} = -P.$$

The distance $R/2$ is termed the *focal length* of the mirror, often written f , while the *power* of the surface is written P . Note that as the object distance s_o goes to ∞ the image distance s_i goes to f .

6.1.4 Refraction in Lenses

Snell's law of refraction is also a good starting point for understanding lenses. Given that all angles are small, indices of refraction n_1, n_2 and a radius of curvature R_{12} , Snell's law implies that

$$\frac{n_2}{s_2} - \frac{n_1}{s_1} = \frac{(n_2 - n_1)}{R_{12}}.$$

(note here that s_1 is negative). If we take the focal length f to be the value of s_2 when s_1 approaches infinity we have

$$f_2 = \frac{n_2 R_{12}}{(n_2 - n_1)}$$

Thus, for refraction, the paraxial equation for image and object distances is

$$\frac{n_2}{s_2} - \frac{n_1}{s_1} = \frac{n_2}{f_2} = -\frac{n_1}{f_1} = P_{12}$$

where P_{12} is the *power* of the surface. The power, like the focal length, measures how strongly converging (or diverging for negative P) an interface is. A plane has zero power.

For a lens in air (or vacuum) we can set $n_1 = 1$ and $n_2 = n$ giving the ratio of the speed of light in vacuum/air to the speed of light in glass, *i.e.* $n = c/c_g$. Snell's law implies that a plane wave front in vacuum/air remains plane as light enters the glass. A typical value for glass is 1.5, so the speed of light in glass is some 200 000 km/s. Since the frequency of light does not change, this means that the wavelength of light is shorter in glass than in vacuum.

An imaging lens is constructed so that the optical length w in all rays is identical even if the geometric distances are different.

6.1.5 Imaging properties

The relation between the distance from a thin lens to an object s and to the image of the object s' is related to the focal length f of the lens by the thin lens formula

$$\frac{1}{s} + \frac{1}{s'} = \frac{1}{f}$$

Note that a point infinitely far away is imaged at the focal point of the lens, *i.e.* that for $s \rightarrow \infty$ then $s' = f$.

Evaluating an optical design is best done by *ray tracing*, *i.e.* by tracing the path of several rays from an object through all the optical elements until they form a final image. This is usually done with a computer program that follows a number of rays, applying Snell's laws and/or the laws of reflection at every interface — usually employing more exact formulations than the paraxial approximation. However, using the paraxial approximation we can get a (useful!) rough estimate using only a ruler, paper and a pencil. *Graphical ray tracing* uses the following specific rules for a thin lens:

1. Rays incident parallel to the axis emerge through the right focal point.
2. Rays incident through the left focal point emerge parallel to the axis.
3. Rays through the vertex do not change direction.

Exercise

2. Follow the rules above to make a figure showing the ray tracing of the image of an arrow (lying in the plane of the sky) through a single lens. Indicate the positions of the object (the arrow), the focal points, and the image of the arrow.

Likewise, when dealing with a spherical mirror

1. Incident rays parallel to the optical axis are reflected through the focal point, F .
2. Incident rays through the focal point are reflected parallel to the axis.
3. Incident rays that reach the vertex are reflected back at an equal and opposite angle.
4. Incident rays through the center of curvature, C , are reflected back upon themselves.

Exercise

3. Follow the rules above for a spherical mirror to make a figure showing the ray tracing of the image of an arrow (lying in the plane of the sky). Indicate the positions of the object (the arrow), the focal point, and the image of the arrow.

6.1.6 Simple telescopes

In its simplest form an astronomical telescope consists of two parts, an objective and an eyepiece. The objective images the object one is studying, and which is “infinitely” far away (parallel rays in) on the focal point or focal plane. This image is real, and can be seen if one places a screen in the focal plane. An eyepiece beyond the focal point functions as a magnifying glass. These two elements form the basic telescope (see figure 2).

The *image scale*, s , describes the mapping of the sky by any camera. The image scale is the angular distance on the sky that corresponds to a unit linear distance in the focal plane of the camera. Given a focal length f , draw paths followed by two rays, one from a point (*e.g.* a star) on the optical axis, the other from a point separated from the first by a small angle θ on the sky. Rays pass through the vertex without deviation, so assuming the paraxial approximation, $\theta \approx \tan \theta$, it is clear that

$$s = \frac{\theta}{y} = \frac{1}{f}$$

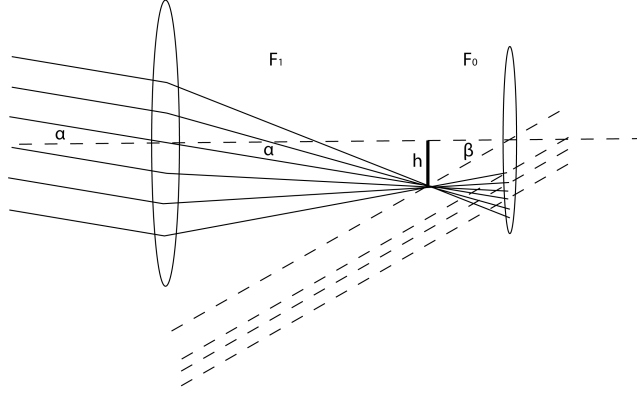


Figure 2: Schematic telescope design. Object has angular size α and is focused by the primary lens with focal length F_1 . Image is observed using the eyepiece adjusted so as to give a virtual image at infinity. The focal length of the eyepiece is F_0 .

where y is the distance the points are separated in the focal plane. Typical focal plane detectors are composed of many identical pixels. If the center of each pixel is separated from its nearest neighbors by d then the *pixel scale* of a telescope is just $s_p = sd$.

Exercise

4. What is the image scale expressed in arcsec per unit length?

The *focal ratio* is defined as

$$\mathcal{R} = \frac{f}{D}$$

where D is the diameter of the entrance aperture of the telescope. One can show that the brightness (energy per unit area to the focal plane) is proportional to \mathcal{R}^2 .

The magnification M of a telescope is given by considering that the image formed by an object at an angle of α (assumed small) to the optical axis. The real image is in focus at distance F_1 , where F_1 is the focal length of the objective lens, since the object is very far away. This image is observed by the eyepiece adjusted so as to give a virtual image at infinity, *i.e.* the eyepiece should be a distance F_0 away from the image formed by the objective. Considering the geometry of the system shown in figure 2 we see that the magnification M must be given by $M = \beta/\alpha$ and that therefore

$$M = \frac{\beta}{\alpha} = \frac{\tan(h/F_0)}{\tan(h/F_1)} \approx \frac{h/F_0}{h/F_1} = \frac{F_1}{F_0}.$$

Note that the image is formed upside down.

6.2 Optical Materials

An ideal mirror should have a reflectivity of 1.0 for all wavelengths (λ) of interest. The substrate should be easy to shape to an accuracy of a fraction of λ , and once shaped, should be mechanically and chemically stable. Low mass is a virtue, as mirrors and lenses should be as large as possible and must be mobile. Since the temperature can change rapidly high thermal conductivity and a low coefficient of thermal expansion are also essential.

For reflecting telescope's first two centuries, one used *speculum metal*, an alloy primarily of copper and tin. However, it was (is) heavy and only has 45% reflectivity at best, and tarnishes easily. Astronomers therefore switched to silvered glass mirrors once the technology became available in the 1880s. Most modern mirrors generally use substrates made with special glasses (*e.g.* Pyrex) or ceramics (Cervit or Zerodur) that have low coefficients of thermal expansion. A coating of Al is best for the near ultraviolet and optical since Al is durable and cheap. Ag is poor in the ultraviolet, is superior to Al when $\lambda > 450$ nm. Au is best in the infrared for $\lambda > 650$ nm. Be is toxic, but is the lowest density workable metal with very good rigidity.

Short wavelengths, extreme ultraviolet (EUV) and shorter, present difficulties: First energetic photons tend to be absorbed, scattered, or transmitted by most materials, and second, curved mirrors in general need to be shaped with an accuracy of at least $\lambda/4$, which for a 1 nm X-ray, amounts to one atomic diameter! X-Ray and EUV focusing telescopes are therefore often designed to operate with grazing incidence as discussed later.

Transmitting materials form lenses, windows, correctors, prisms, filters, fibres, and more. Of primary relevance are index of refraction, dispersion, and absorption. The index of refraction for a number of glasses as a function of wavelength λ is shown in table 1. Generally glasses with a high index of refraction will also have high dispersion and are called “flints”, while those with smaller index and dispersion are called “crowns”.

In ultraviolet (150 nm – 400 nm) ordinary glasses become opaque, fused quartz (SiO_2) is the exception. All other ultraviolet transmitting materials are crystalline, rather than glass, and are more difficult to shape and more likely to chip and scratch. The most useful is perhaps calcium fluoride (CaF_2), which transmits from 160 nm to 7 μm . Other fluoride crystals have similar properties. Fused quartz and fluorides do not transmit well below 180 nm and some birefringent crystals, such as sapphire (Al_2O_3) can be used in the very far ultraviolet. Optics for $\lambda < 150$ nm must be reflecting and for $\lambda < 15$ nm only grazing incidence reflections are possible.

In the infrared ordinary glasses transmit to about 2.2 μm , and some special glasses to 2.7 μm . A large selection of crystalline materials, some identical to those used in the ultraviolet, transmit to much longer λ , but most are soft, or fragile, or sensitive to humidity, so can only be used in protected environments.

Coating the surface of an optical element with a thin film can exploit the wave properties of light to increase, or decrease, its reflectance. A thin film exactly $1/4$ wavelength thick applied to a reflecting substrate will introduce

Refractive index at the specified wavelengths (nm)					
Glass type	361	486	589	656	768
Crown	1.539	1.523	1.517	1.514	1.511
High dispersion crown	1.546	1.527	1.520	1.517	1.514
Light flint	1.614	1.585	1.575	1.571	1.567
Dense flint	1.705	1.664	1.650	1.644	1.638

Table 1: Index of refraction in various glass types vary as a function of wavelength and are thus dispersive.

two reflected beams, one from the front film surface, and the other from film-substrate interface. The second beam will be emerge one-half wavelength out of phase, and the two beams will destructively interfere. If the amplitudes are equal, the interference will be total. An antireflection coating works best at only one wavelength, but will to some extent also work for a broader band centered near the design wavelength. A similar technique can enhance the reflectivity of a surface and multiple layers of alternating high and low index materials can improve the reflectivity of a mirror over a broad range of mirrors. Such *multilayer mirrors* are in frequent use in solar satellites observing the sun at normal incidence in the EUV as will be discussed later.

6.3 Chromatic aberration

Chromatic aberration arises through the change in the refractive index of glass or other optical material with the wavelength. Typical values for some optical glasses are shown in table 1. The degree to which the refractive index varies with wavelength is called the dispersion, and is measured by the constringence ν

$$\nu = \frac{\mu_{589} - 1}{\mu_{486} - \mu_{656}} \quad (2)$$

where μ_{λ} is the refractive index of the wavelength λ . Note that the constringence (also called the *Abbe number* is roughly inversely proportional to the dispersion, *i.e.* $(dn/d\lambda)$. The three wavelengths that are chosen for the definition of ν are those of strong Fraunhofer lines: the C-line 486 nm H β , the D lines 589 nm (Na), and the F-line 656 nm H α . The glasses listed above have constringence that varies from 57 for crown glass to 33 for the dense flint.

The effect of dispersion upon an image is to spread it out into a series of different colored images along the optical axis. Looking at this sequence of images with an eyepiece, then at a particular point along the optical axis, the observed image will consist of a sharp image in the light of one wavelength surrounded by blurred images of varying sizes in the light of all remaining wavelengths. To the eye, the best image occurs when yellow light is focused since it is less sensitive to red and blue light. The spread of colors along the optical axis is called the

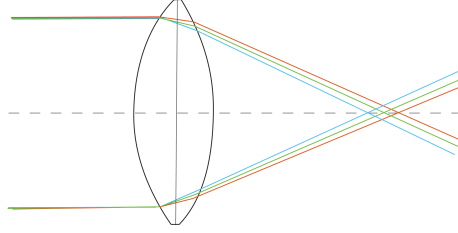


Figure 3: Chromatic aberration.

longitudinal chromatic aberration, while that along the image plane containing the circle of least confusion is called the *transverse chromatic aberration*.

Delayed by Newton's declaration of impossibility, in the 1760s in France and England it was discovered that two (or more) lenses can be combined to reduce the effect of chromatic aberration. Commonly a biconvex crown glass lens is combined with a planoconcave flint glass lens to produce an *achromatic doublet*. This can reduce the chromatic dispersion by a factor 30. If the radii of the curved surfaces are all equal, then the condition for two wavelengths, λ_1 and λ_2 , to have coincident images is

$$2\Delta\mu_C = \Delta\mu_F$$

where $\Delta\mu_C$ and $\Delta\mu_F$ are the differences between the refractive indices at λ_1 and λ_2 for the crown glass and flint glass respectively. More flexibility in the design can be achieved if the two surfaces of the converging lens have differing radii. Then the condition for achromatism is

$$\frac{|R_1| + |R_2|}{|R_1|} \Delta\mu_C = \Delta\mu_F$$

where R_2 is the radius of the surface of the crown glass that is in contact with the flint lens and R_1 is the radius of the other surface of the crown glass lens. Fraunhofer perfected the design and construction of achromats which led to the possibility of making large refractors, which became the telescope design of choice at most observatories after the 1820s. The era of the refractor came to an end around 1900 when the size of these reached roughly 1 m, above which size gravity deforms the shape of the lens. It is interesting to note that the Swedish 1-meter Solar Telescope with a 1.0 m lens is one of the worlds largest refractors.

Since photographic film has a different wavelength sensitivity than the human eye, achromats had to be redesigned when photographic technology was adopted by astronomers in the 1880s.

It is possible to design doublets so that three or more wavelengths are corrected, in this case the corrective lenses are called *apochromats*. Adding more lenses, a properly designed *triplet*, called a *superapochromat* can bring four wavelengths into a common focus.

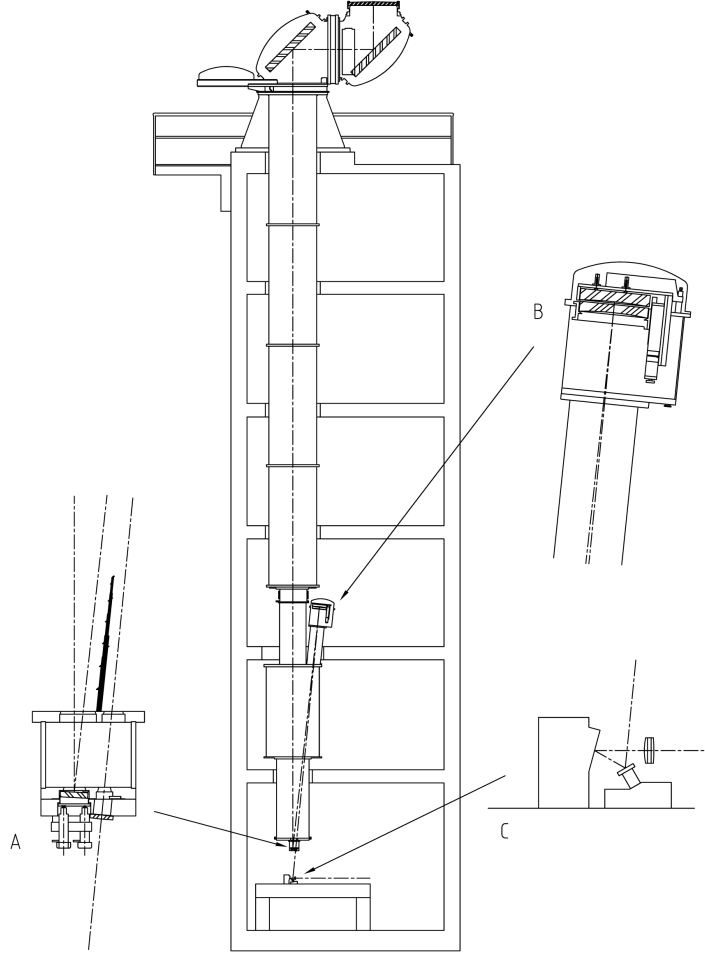


Figure 4: Schematic drawing of the Swedish 1-meter Solar Telescope tower with the turret and vacuum system (center drawing). Details of the box holding the field mirror and field lens are shown in A and the Schupmann corrector with one lens and one mirror in B. The re-imaging optics, located on the optical table and consisting of a tip-tilt mirror, an adaptive mirror and a re-imaging lens are shown in C.

6.3.1 Schupmann achromat

Another interesting solution to the problem of achieving an achromatic image is the combination of a positive lens and a second negative lens in which case one has an intermediate image and the final image is virtual. This is named a Schupmann lens. The drawback of the virtual image location can be overcome with the help of a mirror. The collecting mirror is placed behind the negative

lens, which is used twice and therefore has less power than the negative lens in the usual setup. There are few refracting telescopes in professional night time astronomy, but the Swedish 1-meter Solar Telescope is a refracting telescope in which a Schupmann achromat is used.

6.4 Seidel Aberrations

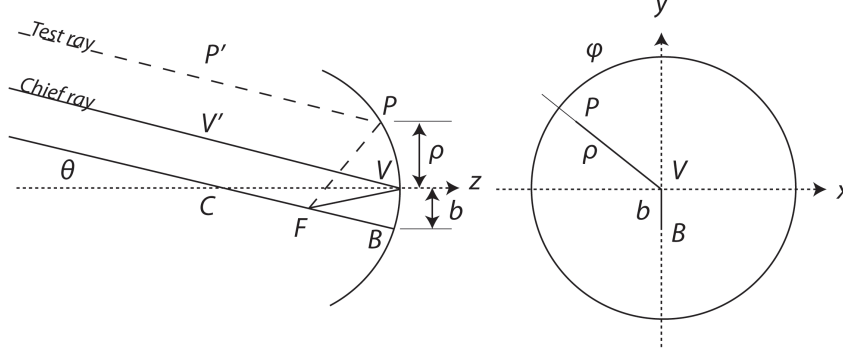


Figure 5: Geometry used in the Seidel aberration discussion. The left hand diagram shows rays through the the center of curvature (CFB) and vertex (VV', the chief ray), which along with the optical axis defines the meridional plane. Point P is outside the plane of the diagram. The right hand locates points P, V, and B in the plane of the aperture when looking down the optical axis.

Consider a “perfect” telescope, it should transform an incident plane wavefront into a converging spherical wavefront whose center is the focus predicted by the paraxial approximation. For point sources off-axis the perfect telescope should produce spherical wavefronts converging somewhere on the image plane, also as predicted by the paraxial theory. Define the *chief ray* as the one passing from the object through the center of the entrance aperture. The plane containing this ray and the optical axis defines the *meridional* or *tangential plane*. The plane perpendicular to this plane is called the *sagittal plane*. If we now analyse the angles of reflection or refraction for a curved surface using the approximation

$$\sin \theta \approx \theta - \frac{\theta^3}{3!}$$

one obtains *third-order aberration theory* which is much more accurate than that given by paraxial theory where one assumes $\sin \theta = \tan \theta = \theta$. In this treatment one can show that the optical path *difference* between a test ray and the chief ray takes the form

$$\Delta w(\rho, \phi, b) = C_1 \rho^4 + C_2 \rho^3 b \cos \phi \quad (3)$$

$$+ C_3 \rho^2 b^2 \cos^2 \phi + C_4 \rho^2 b^2 + C_5 \rho b^3 \cos \phi \quad (4)$$

where the C_i values depend on the shapes of the optical surfaces and/or the indices of refraction. Each of the terms in this equation 3 has a different functional dependence, so one distinguishes five monochromatic third-order aberrations which are also known as the *Seidel aberrations*. Note that since the range of ρ depends on the diameter of the telescope the terms with the highest order of ρ are the most important.

6.4.1 Spherical aberration $\propto \rho^4$

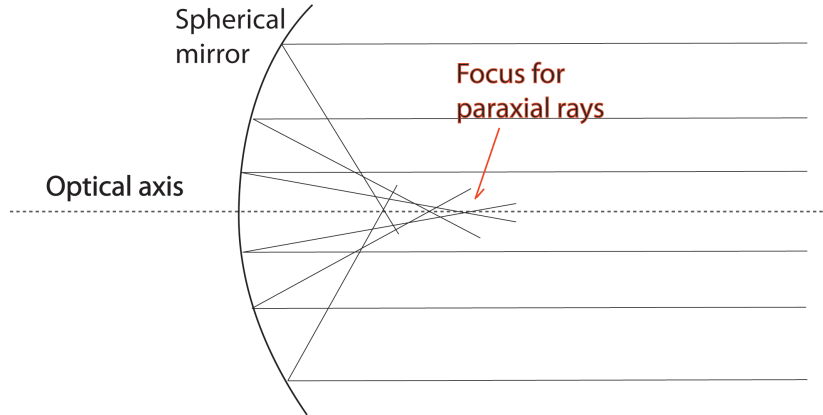


Figure 6: Spherical aberration.

A common and severe aberration of both lenses and mirrors is *spherical aberration*: annuli of the lens or mirror that are of different radii have different focal lengths. It is possible to minimize but not eliminate spherical aberration by minimizing the angles of incidence on every surface. Likewise, any lens with a large enough focal ratio will approach the paraxial case closely enough that the blur due to spherical aberration can be made smaller than the seeing disk. Since a large focal ratio also minimizes the chromatic aberration, early refracting telescopes (1608 – 1670) tended to have moderate apertures and large focal lengths, at the cost of reduced image brightness and unwieldy telescope length.

For mirrors, removing spherical aberration is simple. A paraboloid reflector, made by deepening the sphere to a paraboloidal surface, will display no on-axis aberrations at all — rays from infinity parallel to the axis will all come to the same focus. Newton constructed the first workable reflecting telescope in 1668, and reflecting telescopes were fashionable from the 1780s (when the Herschels were making great discoveries with speculum paraboloids) until the superiority of the refractor became apparent in the 1830s as a result of the discovery that an achromatic doublet can be designed to minimize both chromatic aberration and spherical aberration: These cannot be eliminated from a simple lens without using aspheric surfaces, but can be reduced for a given focal length by adjusting

the shape factor q

$$q = \frac{R_2 + R_1}{R_2 - R_1}$$

where R_1 and R_2 are the radii of the first and second surfaces of the lens respectively. Judicious choice of surface radii in an achromatic doublet can lead to some correction of spherical aberration while still retaining the color correction.

It is also possible to remove spherical aberration from a *spherical* mirror by the use of a transparent corrector plate, as we will discuss in connection with Schmidt and Maksutov telescopes later in this lecture.

6.4.2 Coma $\propto \rho^3 b \cos \phi$

Coma in an optical system refers to an aberration which results in off-axis point sources such as stars appearing distorted. Specifically, coma is defined as a variation in magnification over the entrance pupil. Coma is an inherent property of telescopes using parabolic mirrors, thus deepening a spherical mirror in order to correct spherical aberration will introduce coma. It causes the images for objects away from the optical axis to consist of a series of circles that correspond to the various annular zones of the lens or mirror and which are progressively shifted away from the optical axis. The severity of the coma is proportional to the square of the aperture and the angular size of the blur is given by

$$L = A \frac{bD^2}{f^3} = A\theta\mathcal{R}^{-2}$$

where A is a constant that depends on the shape of the surface.

Lenses or mirrors in which both spherical aberration and coma are minimized at a single wavelength are called best form or *aplanatic*. No single element aplanatic telescope is possible, either in a reflector or a refractor. As with spherical aberration, a large focal ratio will reduce coma, but impose penalties in image brightness and telescope length. Otherwise, minimizing coma in a refracting system requires a system of lenses, and at least two mirrors in reflecting telescopes.

6.4.3 Astigmatism $\propto b^2 \rho^2 \cos^2 \phi$

Astigmatism is an effect where the focal length differs for rays in the plane containing an off-axis object and the optical axis (tangential plane), in comparison with rays in the plane at right angles to this (sagittal plane). An example of astigmatism is shown in figure 7. The angular dependence suggests that the wavefront distortion is zero for rays in the sagittal plane (*i.e.* $\phi = 90^\circ$, $\phi = 270^\circ$), but an extremum for rays in the meridional plane.

The blurred image suffering astigmatism has an angular length

$$L = B\theta^2\mathcal{R}^{-1}$$

Astigmatism

Different focal planes.

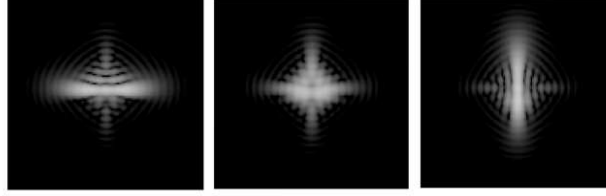


Figure 7: Example of the effect of astigmatism.

where B is a constant that depends on the shape of the reflecting or refracting surface.

It is possible to correct astigmatism, but at the expense of introducing an aberration called field curvature, *i.e.* that the surface containing the sharply focused image is not flat but curved. A system where a flat image plane is combined with corrected astigmatism is termed *anastigmatic* and a telescope that corrects for astigmatism, coma, and spherical aberration is anastigmatic aplanat.

6.4.4 Field curvature $\propto \rho^2 b^2$

This aberration results from off-axis images falling on a spherical surface called the *Petzval surface*. Detectors are generally flat, so much of an image formed on a detector will be out of focus. For a small detector, this defocus will not exceed the seeing disk or diffraction limit and therefore not be a problem. For larger detectors is to bend the detector to fit the Petzvel surface, as was done with photographic plates using a mechanical plate holder. Large solid-state detectors like CCDs are mechanically quite fragile, so bending is not an option. In which case a corrector plate or lens is used to flatten the field.

6.4.5 Distortion $\propto \rho b^3 \cos \phi$

The final aberration is *distortion*, which is a variation in the magnification over the image plane. A distorted system will deliver images that suffer *pincushion* or *barrel* distortion according to whether the magnification increases or decreases with distance from the optical axis.

Since distortion does not change the image quality, it can be removed from digital in a post processing phase.

Another fault of optical systems is called *vignetting*. It arises as a result of uneven illumination of the image plane, usually due to the obstruction of the light path by parts of the instrument.

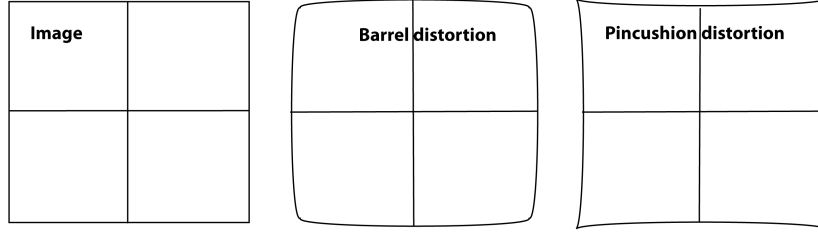


Figure 8: Distortion

6.4.6 Zernike polynomials

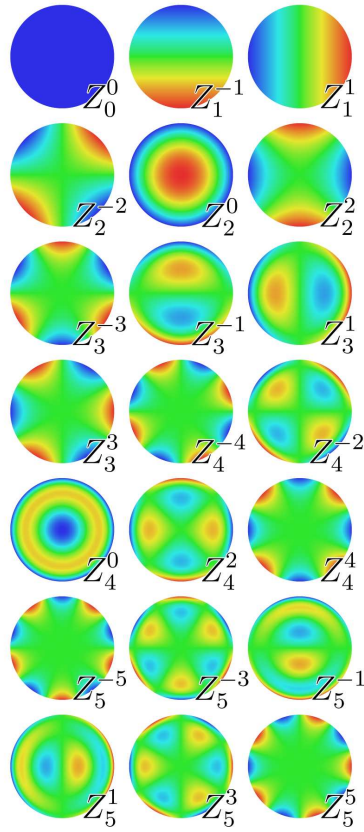


Figure 9: The first few Zernike polynomials, see table 2

In an optical system the location of the diffraction focus will depend on the type and magnitude of aberration present. Because of this dependence, it is

Roles of the Zernike polynomials

a_0	“Piston”, equal to the mean value of the wavefront
$a_1 \times \rho \cos(\varphi)$	“X-tilt”, the deviation of the overall beam in the sagittal direction
$a_2 \times \rho \sin(\varphi)$	“Y-tilt”, the deviation of the overall beam in the tangential direction
$a_3 \times (2\rho^2 - 1)$	“Defocus”, a parabolic wavefront resulting from being out of focus
$a_4 \times \rho^2 \cos(2\varphi)$	“X-astigmatism”, horizontally oriented cylindrical shape
$a_5 \times \rho^2 \sin(2\varphi)$	“Y-astigmatism”, vertically oriented cylindrical shape
$a_6 \times (3\rho^2 - 2)\rho \cos(\varphi)$	“X-coma”, comatic image flaring in the horizontal direction
$a_7 \times (3\rho^2 - 2)\rho \sin(\varphi)$	“Y-coma”, comatic image flaring in the vertical direction
$a_8 \times (6\rho^4 - 6\rho^2 + 1)$	“Third order spherical aberration”

Table 2: ρ is the normalized pupil radius, φ is the azimuthal angle around the pupil, the coefficient a_0, \dots, a_8 are the wavefront errors in wavelengths.

appropriate to restructure the classical aberration terms and include explicitly the required image shift to place the diffraction focus at the origin. These modified terms are called the orthogonal aberrations, with polynomials in ρ and φ (*i.e.* using a circular co-ordinate system) called *Zernike polynomials*. Developed by Frits Zernike in the 1930s, Zernike’s polynomials are orthogonal over a circle of unit radius. A complex, aberrated wavefront profile may be curve-fitted with Zernike polynomials to yield a set of fitting coefficients that individually represent different types of aberrations. Their advantage are the simple analytical properties which leads to closed form expressions of the two-dimensional Fourier transform in terms of Bessel functions. Their disadvantage, in particular for high n is the unequal distribution of nodal lines over the unit disk, which introduces ringing effects near the perimeter $\rho \approx 1$, which leads attempts to define other orthogonal functions over the circular disk¹.

There are even and odd Zernike polynomials. The even ones are defined as

$$Z_n^m(\rho, \varphi) = R_n^m(\rho) \cos(m\varphi)$$

and the odd ones

$$Z_n^{-m}(\rho, \varphi) = R_n^m(\rho) \sin(m\varphi)$$

where m and n are non-negative integers with $n \geq m$, φ is the azimuthal angle and ρ is the normalized radial distance. The radial polynomials R_n^m are defined

¹For atmospheric turbulence Zernike polynomials are not the optimal set of basis functions because the Zernike coefficients are statistically dependent. Basis functions that do not have this property can be constructed and are called the *Karhunen–Loève functions* which represent stochastic processes as an infinite linear combination of orthogonal functions analogous to a Fourier series representation of a function on a bounded interval. The coefficients in the Karhunen–Loève theorem are random variables and the expansion basis depends on the process. The Karhunen–Loève transform adapts to the process in order to produce the best possible basis for its expansion. (Source: Wikipedia and Gua-ming Dai *Modal compensation of atmospheric turbulence with the use of Zernike polynomials and Karhunen–Loève functions* J.Opt.Soc.Am. 12, October 1995.)

as

$$R_n^m(\rho) = \sum_{k=0}^{(n-m)/2} \frac{(-1)^k (n-k)!}{k! [(n+m)/2 - k]! [(n-m)/2 - k]!} \rho^{n-2k} \quad \text{if } n-m \text{ even}$$

$$R_n^m(\rho) = 0 \quad \text{if } n-m \text{ odd}$$

The first few Zernike polynomials are described in table 2.

6.5 Practical telescopes

Even after a telescope design has been perfected; in which one attempts to remove as many of the aberrations as possible from the list above, there remains the task of physically producing the instrument specified. This must be done taking into consideration what one actually needs to observe in order to meet a certain scientific goals.

Manufacturing of lenses and mirrors is broadly similar: the surface is roughly shaped by moulding or diamond milling. It is then matched to another surface formed in the same material whose shape is inverse, called the *tool*. The two surfaces are ground together with coarse carborundum or other grinding powder between them until the required surface begins to approach its specifications. The pits left behind are removed by a second grinding stage in which finer powder is used. A third stage follows, and so on. As many as eight or ten such stages may be necessary. When grinding pits are reduced to a micron or so in size, the surface may be polished. Once the surface has been polished it can be tested for accuracy of fit. A third stage termed *figuring* is often necessary when the surface is not within specification.

There are a number of tests that can determine the shape of a mirror's surface to within ± 50 nm or better, such as Foucault, Ronchi, Hartmann and Null tests.

Epicyclic grinding. Larger mirrors are ground by using large machines that move the tool in an epicyclic fashion. The motion of the tool is similar to that of the planets under the Ptolemaic model of the solar system. The epicyclic motion can be produced by a mechanical arrangement, but commercial production of large mirrors is now largely done by computer controlled planetary polishers.

Stressed polishing. The mirror segments for large instruments such as the 10 m Keck or Gran Tecan telescopes are small, off-axis parts of the total hyperbolic shape. These are produced by so-called stressed polishing where the blank is deformed by carefully designed forces from a warping harness, and then polished to a spherical shape. When the the deforming forces are released the blank springs into the required shape.

Numerically controlled diamond milling. The requirements for for non-axisymmetric mirrors for segmented mirror telescopes and and for glancing incidence x-ray telescopes have led to the development of numerically controlled diamond milling machines which can produce the required shaped and polished surface directly to an accuracy of 10 nm or better.

The defects in an image that are due to surface imperfections on a mirror will not exceed the Rayleigh limit if those imperfections are less than one eighth of the wavelength of the radiation for which the mirror is intended. The restriction on lenses is about twice as large as those of a mirror since the ray deflection is distributed over two faces.

The surface must normally receive its reflecting coating after production. The vast majority of astronomical mirror surfaces have a thin layer of aluminium evaporated on to them by heating aluminium wires suspended over the mirror inside a vacuum chamber. Other materials such as silicon carbide are sometimes used, especially for UV since the reflectivity of aluminium falls for < 300 nm. Aluminium initially has a reflectivity of 90 %, but this will fall to 75 % in the matter of months, hence realuminization is needed regularly. Mirrors coated with suitably protected silver can achieve 99.9 % reflectivity in the visible, and this may be required as the total number of reflections becomes large.

Coefficient of thermal expansion. To avoid deformations of its shape it is essential that the coefficient of thermal expansion for a mirror is low. For glass it is of order 9×10^{-6} K $^{-1}$, for pyrex 3×10^{-6} K $^{-1}$, and for fused quartz 4×10^{-7} K $^{-1}$. Pyrex has been the favorite material up until the last 30 years when quartz or artificial materials such as ‘CerVit’ or ‘Zerodur’. Another possibility is to use materials with a very high thermal conductivity, such as silicon carbide, graphite epoxy, steel beryllium, or aluminium. However, it can be very difficult to polish these materials as they have a relatively coarse crystalline surface.

Rigidity of mirrors, thin mirrors and honeycomb mirrors. Small solid mirrors can maintain their shape simply by mechanical rigidity. However, the thickness required for such rigidity scales as the cube of the size, so the weight of a solid mirror scales as D^3 — this quickly becomes too expensive to build. There are various ways to reduce the weight of mirrors, these fall into two major classes: thin mirrors and honeycomb mirrors. Thin mirrors are also subdivided into monolithic and segmented mirrors. In both cases active support is needed in order to maintain the correct shape. Honeycomb mirrors are thick solid blanks that have had a lot of the material behind the reflecting surface removed, leaving only thin struts to support that surface.

Rotating mirrors, bath of mercury. Isaac Newton realized that the surface of a steadily rotating liquid would take up a paraboloidal shape under the combined forces of gravity and centrifugal acceleration. If the liquid reflects light, like mercury, gallium, gallium-indium alloy, or an oil suffused with reflecting particles, one can then use it as the primary mirror of a telescope.

6.5.1 Designs

The most common format for large telescopes is the Cassegrain system, although most large telescopes can be usually be used in several alternative different modes by interchanging the secondary mirrors. The Cassegrain is based on a paraboloidal primary and a convex hyperboloidal secondary. The major advantage of the Cassegrain lies in its telephoto characteristic, the secondary mirror serves to expand the beam from the primary mirror so that the effective

focal length of the whole system is several times the that of the primary. A compact (thus cheap) mounting can thus be used to hold the optical elements while retaining the advantages of long focal length and large image scale. The Cassegrain is afflicted with coma and spherical aberration to about the same degree as an equivalent Newtonian.

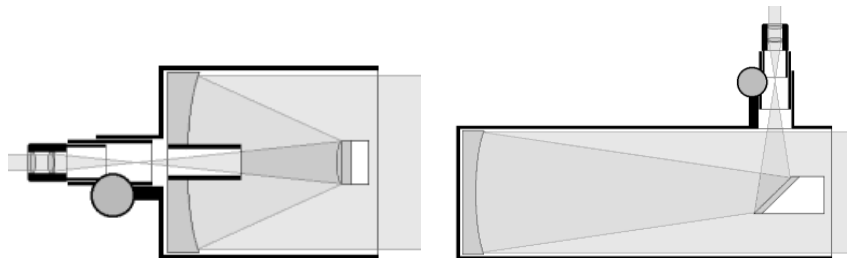


Figure 10: Cassegrain and Newtonian Designs

A great improvement of the Cassegrain can be achieved by a slight alteration to a Ritchey-Chrétien system. The optical arrangement is identical but for that the primary mirror is deepened to a hyperboloid and a stronger hyperboloid is used for the secondary. With this system both coma and spherical aberration can be corrected and one achieves a aplanatic system.

Corrector lenses just before the focus. One can also improve Cassegrain or Ritchey-Chrétien systems by adding correctors just before the focus. The correctors are low power lenses whose aberrations oppose those of the main system. The corrective optics may be combined with a focal reducer to enable the increased field of view to be covered by the detector array. A focal reducer is a positive lens, usually a apochromatic triplet, placed just before the focal point of the telescope that decreases the effective focal length and so gives a smaller image scale.

Coudé focus. Another related telescope design is the Coudé system, which in effect is a very long focal length Cassegrain or Ritchey-Chrétien whose light beam is folded and guided by additional flat mirrors to give a focus whose position is fixed irrespective of the telescope position. One way is to insert a diagonal mirror after the secondary, light is reflected down the declination, and then down the polar axis by a second diagonal mirror. Light then always emerges from the end of the polar axis, whatever part of the sky the telescope is inspecting.

Nasmyth focus/system. With alt-ax mountings the light beam can be directed along the altitude axis to one of the two Nasmyth foci on the side of the mounting. These foci still rotate as the telescope changes azimuth, but this is still easier than changing the altitude and altitude of a conventional Cassegrain focus. Both of the fixed focus systems, Coudé and Nasmyth, are very advantageous when large equipment such as high dispersion spectrographs, are to be used. Disadvantages are that the field of view rotates as the telescope tracks

an object across the sky, and is very small due to the large effective focal ratios that are required to bring the focus through the axes, and finally the additional reflections cause the loss of light.

The simplest of all designs is a mirror used at its prime focus. That is, the primary mirror is used directly to produce the images and the detector is placed at the top end of the telescope. The image quality at the prime focus is usually poor even a few tens of arcsec away from the optical axis because the primary mirror's focal ratio may be as short as $f/3$ or less in order to reduce the instrument length. A system that is almost identical to the use of a telescope at prime focus is the Newtonian. A secondary flat secondary mirror is used just before the prime focus. This reflects the light beam to the side of the telescope from where access to it is relatively simple. There is little advantage to this design over use of the prime focus for large telescopes. The images in a Newtonian system and at prime focus are very similar and are of poor quality away from the optical axis.

A Gregorian is similar to the Cassegrain except that the secondary is a concave ellipsoid and is placed after the prime focus. Since the primary mirror creates an actual image before the secondary mirror, the design allows for a field stop to be placed at this location, so that the light from outside the field of view does not reach the secondary mirror. This is a major advantage to solar telescopes, where a field stop can reduce the amount of heat reaching secondary mirror and subsequent components. Hinode/SOT (Solar Optical Telescope) is an example of a Gregorian.

Refractors (and the Swedish 1-meter Solar Telescope).

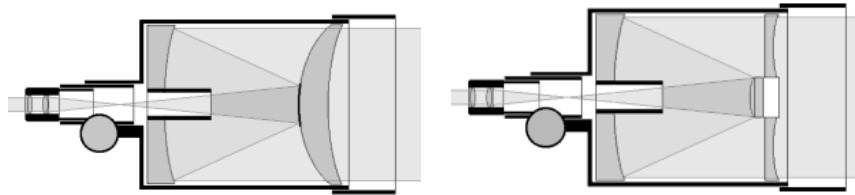


Figure 11: Maksutov and Schmidt-Cassegrain Designs

The catadioptric (from catoptric, *ie* reflecting, and dioptric, *ie* refracting) group of which the Schmidt camera is best known. A catadioptric system uses both lenses and mirrors in its primary light gathering section. Very high degrees of corrections of the aberrations can be achieved because of the wide range of variable parameters that become available. Diffraction limited performance over fields of view of several degrees is possible with focal ratios as fast as $f/1.5$ or $f/2$. The Schmidt camera cannot be used visually since its focus is inaccessible. One of the best modifications of this is the Maksutov. A similar system is the Schmidt-Cassegrain telescope.

6.5.2 Mountings

The functions of a telescope mounting are to hold the optical components in their correct mutual alignment, and to direct the optical axis towards the object to be observed. One can consider the functions of the mounting under three separate aspects: supporting the optical components, preserving their correct spatial relationship, and acquiring and holding the object of interest in the field of view.

Equatorial mounting. This is a two axis mounting, with one axis, the polar axis, aligned parallel with the Earth's rotational axis, and the other, the declination axis, perpendicular to the polar axis. Only a single constant velocity motor is required to rotate the mounting around the polar axis in order to track an object.

Alt-az mounting. This mounting has motions in altitude and azimuth. Structurally it is much simpler and much more compact than the equatorial system. Its drawbacks are that the field of view rotates telescope motion, and that it needs driving continuously in both axes and with variable speeds in order to track an object.

Fixed position telescopes. Some telescopes do not track: *e.g.* transit telescopes point only along the meridian. Other telescopes do not vary their pointing at all and the tracking function is realized by moving the detector in the image plane while the massive telescope remains stationary.

Coelostat and heliostat. A coelostat is comprised of two flat mirrors that are driven so that a beam of light from any part of the sky is routed into a fixed direction. They are particularly used in conjunction with solar telescopes whose extremely long focal lengths make them impossible to move. One mirror of the coelostat is mounted on a polar axis and driven at half the sidereal rate. The second mirror is mounted and driven to reflect the light into the fixed telescope.

Mountings in space. Telescopes in space must also mount and track but since the effects of gravity are much less some aspects of these tasks is easier. In general two methods are used to stabilize the orientation of a telescope in space: small rockets and spinning reaction wheels. A space telescope often has more stringent pointing requirements than a telescope on the ground, and a guide star is often used to achieve this precision. To point on a given target requires continuous telescope movement because of the aberration of starlight induced by the telescopes orbital velocity and because of torques induced by atmospheric drag and thermal effects.

6.5.3 Telescopes in space

In connection with a RAND project in 1946, Lyman Spitzer was asked to consider the advantages of putting an astronomical telescope in space. This work came to full fruition in 1990 when the Hubble Space Telescope (HST) was launched. The HST has an aperture of 2.4 m and has generated unprecedented results, revolutionizing astronomy. Its replacement is meant to be the 6.5 m James Webb Space Telescope (JWST) built by NASA and ESA in col-

laboration and to be placed at the Sun-Earth L₂ Lagrange point in 2017 (or so).

The absence of an atmosphere and hence wavefront distortions means that a space telescope should have diffraction limited resolution. *I.e.* that the “diameter” of a star will be of order the Airy disk

$$\theta = \frac{2.44\lambda}{D}$$

where λ is the wavelength observed and D the diameter of the telescope. Since there are no other distortions, the precision and alignment of optical surfaces becomes especially critical in space, where seeing will not mask any errors.

Note that the Earth’s atmosphere is itself a source of background light, so from space the background is lower than on the ground. On the ground there are several sources: *airglow* (atomic and molecular line emission from the upper atmosphere), scattered sunlight, starlight and moonlight, and scattered artificial light. In the infrared, the atmosphere and telescopes both glow like blackbodies and dominate the background. From space the main contributor in the visible and in the near infra-red (NIR) comes from sunlight scattered from interplanetary dust (visible in dark sites on the ground as *zodiacal light*.) In the V band, the darkest background for the HST (near the ecliptic poles) is about 23.3 magnitudes/arcsec², while at the darkest ground based site it is of order 22.0 magnitudes/arcsec². In the thermal infrared the sky from space can be much darker than on the ground because it is possible to keep the telescope quite cold in space.

The atmosphere absorbs light at certain wavelengths, at these wavelengths it is only possible to observe from space. This is especially true for gamma-ray, x-ray, and UV astronomy, but also at other wavelengths: the atmosphere is a dynamic system and weather happens! Astronomers are often happy to achieve 1% accuracy on the ground, from space photometry precise to one part in 10⁵ is possible.

A space telescope in an orbit far enough away from the Earth (and the Moon) also has access to the entire sky all the time, half the sky is not blocked by the Earth at any given time, nor is a space telescope hindered by the day-night cycle or by moonlight.

A telescope on the ground experiences changing gravitational stresses as in points in different directions, and will respond by changing shape. Stresses induced by wind and temperature changes generate similar problems. Most of the expense of a large modern telescope is not in the optics, but in the systems needed to move and shelter the optics, while maintaining figure and alignment.

However, the total optical/infrared aperture on the ground exceeds that in space by a factor of at least 200, and that factor is likely to increase in the near future. The disadvantages of space astronomy are led by its enormous cost. Typically the two 8 m Gemini telescopes had a construction budget of 100 MUSD, the 2.4 m HST cost 2000 MUSD to construct and launch.

6.5.4 Observatory engineering

1. The location of an observatory is vital to its success. Seeing is substantially better at high altitude on isolated islands like Mauna Kea and La Palma and the various sites in northern Chile.
2. Lightweight mirrors in a compact structure are cost effective. Modern primary mirrors have fast focal ratios: $f/1.75$ for Keck, $f/3.3$ for Hale, which means shorter telescope length and a smaller building. The same is true for altazimuth mounts compared to equatorial mounts.
3. Active optics can improve image quality.
4. Local climate control can improve natural seeing. Structures that permit substantial airflow with *e.g.* fans, louvres, retractable panels, while still protecting from wind buffeting can improve seeing appreciably.
5. Novel focal arrangements can reduce costs of specialized telescopes. Keck and VLT can combine beams from several telescopes at a common focus (*i.e.* interferometry).
6. Adaptive optics can eliminate some of the effects of atmospheric seeing.

6.5.5 Future telescopes

If adaptive optics can produce a large diffraction limited FOV, then current mirror and mounting technology can allow telescopes of up to 100 m diameters. At present (2010) there are three serious multinational projects to build single aperture telescopes larger than the currently operational 8 – 11 m instruments. All three projects expect to see first light around 2018; and include the European Extremely Large Telescope (www.eso.org/sci/facilities/eelt) with a primary of $D = 42$ m built up of 1000 1.4 m segments, the Giant Magellan Telescope (www.gmto.org) $D = 24.5$ m of 7 8.4 m segments, and the Thirty Meter Telescope (www.tmt.org) $D = 30$ m consisting of 492 1.4 m segments. Each of these telescopes has a cost of some 10^9 US dollars.